PHOTONICS Research

Optofluidics in bio-imaging applications

Sihui Chen, Rui Hao, Yi Zhang, and Hui Yang*

Laboratory of Biomedical Microsystems and Nano Devices, Bionic Sensing and Intelligence Center, Shenzhen Institutes of Advanced Technology, Chinese Academy of Sciences, Shenzhen 518055, China
**Corresponding author: hui.yang@siat.ac.cn*

Received 22 January 2019; revised 5 March 2019; accepted 5 March 2019; posted 7 March 2019 (Doc. ID 357818); published 17 April 2019

Bio-imaging generally indicates imaging techniques that acquire biological information from living forms. Recently, the ability to detect, diagnose, and monitor pathological, physiological, and molecular dynamics is in great demand, while scaling down the observing angle, achieving precise alignment, fast actuation, and a miniaturized platform become key elements in next-generation optical imaging systems. Optofluidics, nominally merging optic and microfluidic technologies, is a relatively new research field, and it has drawn great attention since the last decade. Given its abilities to manipulate both optic and fluidic functions/elements in the micro-/nanometer regime, optofluidics shows great potential in bio-imaging to elevate our cognition in the subcellular and/or molecular level. In this paper, we emphasize the development of optofluidics in bio-imaging, from individual components to representative applications in a more modularized, systematic sense. Further, we expound our expectations for the near future of the optofluidic imaging discipline.

https://doi.org/10.1364/PRJ.7.000532

1. INTRODUCTION

Imaging is defined as the representation or reproduction of an object's appearance and structure. Human beings perceive and communicate with the world mostly based on vision, which normally uses light as the medium to convey and express information. In the aspects of the developing pathology, physiology, and therapeutics, people utilize a wide variety of imaging media/modalities to harvest multidimensional parameters from living organisms: from the metabolic and anatomical level (computed tomography/magnetic resonance imaging/ultrasound) down to the single-cell and even single biomolecular level [atomic force microscopy (AFM)/fluorescent microscopy/electron microscopy] [1–3]. Nowadays, together with optical techniques, bio-imaging has not only enabled us to dig biological information deep inside our bodies, but also revolutionized the way we understand, detect, and treat diseases in different angles and dimensions.

Today, we are experiencing fast changes in personal health management: from the present one-fits-all post-medical care to targeted therapy based on genetics or molecular mechanisms in different time frames [4]. Accordingly, the major task of imaging techniques in biological research now relies on detecting, diagnosing, and monitoring molecular dynamics in terms of pathology and physiology, which will benefit early diagnosis, prognosis, and disease monitoring [5]. Therefore, the most pivotal step is generating a customized imaging system that can track the temporal/spatial distribution of targeted molecules and interrogate their behavior at the cellular/subcellular level. However, most anatomical imaging modalities have come close to practical limits on spatial resolution. In fact, image quality has improved so dramatically that any further increments may prove to be of only marginal value. Also, the compatibility between biological samples and imaging instruments is another crucial concern, for example, electron microscopy and AFM usually require complex sample preparation steps when they are used to study biological samples.

To meet with such challenges, the so-called optofluidic technology has drawn much focus in recent years. Optofluidics, namely, bridging "optics" and "microfluidics," is capable of manipulating light with on-chip fluidic processes, or using light to control fluidic entities. However, recent efforts on optofluidics have already pushed the technology forward and exceeded its original definition. Nowadays, either using fluidic and optical elements synergistically, or employing advanced optical/photonic methods on a microfluidics platform to concretize enhanced deployment, reliability, accuracy, and throughput, especially in the on-chip aspect, can be defined as optofluidics [6]. In the past decade, optofluidics-based flow cytometry [7,8], interferometry [9], and Raman spectroscopy [10] proved their potential in cell studies and molecular imaging. Benefiting from advantages of microfluidics such as low consumption, micro-/nanoscale sample manipulation, and compatibility with consumer electronics, optofluidic imaging also offers various scenarios in personalized medicine [5].

Previously published review papers either summarized the working principles of specific optical components (e.g., laser [11] and lens [12]), or illustrated applications of optofluidic technologies in different areas (e.g., biosensors [13], on-chip manipulation of cells [14]). However, regarding bio-imaging, few papers have been dedicated to systematically discussing the

implementation of optofluidics in the sense of composing a compact imaging platform. Besides, the definition of optofluidic imaging is sometimes confused with that of imaging with microfluidic devices in some papers. Thus, it is needed to provide a comprehensive demonstration of the evolution of optofluidic bio-imaging. This paper starts with the composition of a basic optofluidic imaging tool (e.g., laser, prism, switch, lens) for innovative on-chip optical imaging methods, aiming to sketch a blueprint of today's optofluidic imaging systems. We further demonstrate on-chip sample handling and imaging data acquisition methods as extensions for a fully integrated optofluidic system. Finally, we provide our perspective on optofluidic bio-imaging, especially on how this technology will impact modern biological studies.

2. OPTOFLUIDIC COMPONENTS

Back in the 18th century, the interaction of fluid and light had already inspired the invention of the liquid mirror telescope, which used a liquid to replace traditional optical components. Although it sowed the seed for optofluidics, the term "optofluidics" itself had not been exploited until the first decade of 2000s [15]. Along with the development of microfluidic technologies, researchers also improve lab-on-a-chip functionalities by incorporating optical components into the same system. Most solid-phase optical components lack the capabilities of deformation and position adjustment, as they are usually fixed in an integrated system. On the contrary, fluid-based optical components can achieve self-tunability, adaptivity, and precise alignment in the context of optofluidic circuits. In the following years, the number of papers regarding "optofluidics" experienced a boom with a wide variety of applications such as bio-chemical sensors [13], bio-imaging [16], energy production and harvesting [17], and on-chip manipulation of cells [14,18].

Many research groups have presented a large collection of optofluidic components for imaging. These optofluidic components are categorized in terms of either their working mechanisms or their functions similar to their macroscale counterparts (e.g., waveguide, lens, cavity) [19]. In 2013, Zhao *et al.* summarized four major components, namely, an optofluidic laser, a prism, a switch, and a lens, to compose an optofluidic system to fulfil the requirements of imaging [20]. In the same framework, we will present the working principles of these optofluidic components, and focus on their timely progresses and challenges in this section.

A. Optofluidic Lasers

The first-generation microfluidic laser based on a Fabry–Perot resonator was developed by Whitesides' group [21]. In this work, fluorescence was constrained in the core flow of an optofluidic waveguide. Both ends of the waveguide were coated with a thin layer of gold, acting as reflecting mirrors. Therefore, the fluorescence bounced back and forth and escaped from the gold layer, forming a laser. The aspects of emission wavelength, numerical aperture (NA), and absorbance of this laser system can be configured by changing the dye/solvent composition and the flow rates of the core/cladding layer. Further, an optofluidic laser based on distributed-feedback (DFB) gratings was proposed in Ref. [22]. As shown in Fig. 1(a), an SU-8 pattern with a high refractive index (RI) (i.e., a DFB resonator) is

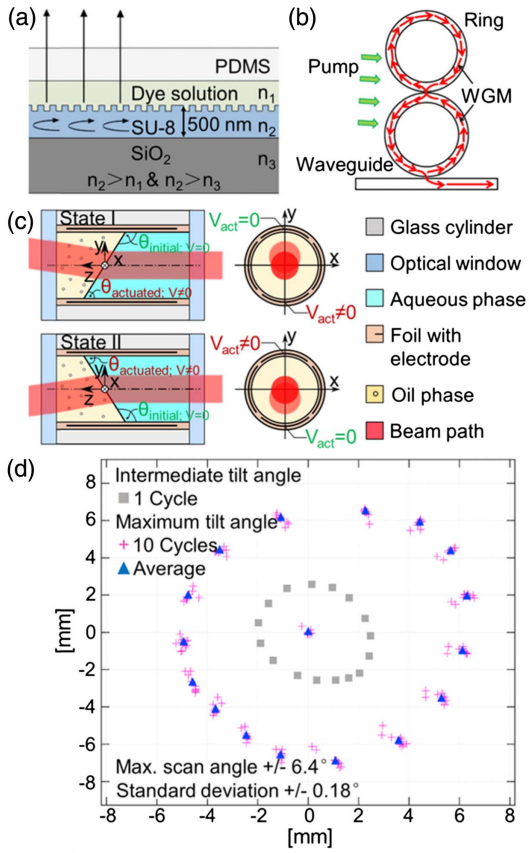

Fig. 1. (a) DFB resonator-based optofluidic laser. (b) An optofluidic ring resonator laser. (c) A rotatable optofluidic prism with beam positions tuned by the electro-wetting effect. (d) Beam positions of the tunable prism for 10 repeated cycles. Maximum tilt angle (pink crosses), spatial average (blue triangles), and the smaller tilt angle (gray squares) are shown in the figure. (a) Reproduced with permission [22], Copyright 2009, American Institute of Physics. (b) Reproduced with permission [24], Copyright 2011, American Institute of Physics. (c), (d) Reproduced with permission [29], Copyright 2016, Optical Society of America.

sandwiched between a cladding flow and a silicon dioxide layer. The DFB grating has a relatively large surface area and allows enhanced interaction of the evanescent tail with the upper liquid gain medium, forming a surface-emitting optofluidic laser via output coupling.

Although single-mode operation and a large tunable wavelength range have been realized with the above two types of optofluidic lasers, the relatively low Q factors ($\sim 10^3$) prevent them from achieving low lasing thresholds [23]. As a comparison, an optofluidic ring resonator (OFRR) laser system can achieve a high Q factor; a schematic of an OFRR laser is shown in Fig. 1(b). The system consists of two mismatched ring resonators and a liquid-filled waveguide [24]. The lower ring is optically coupled with the straight waveguide but physically disconnected. A water-based medium with a fluorescent dye is filled into the structures. Fluorescent light produced upon excitation is confined in the gain medium because of the low-RI polydimethylsiloxane (PDMS) sidewalls, and is emitted through the waveguide. The optical coupling between the two OFRRs and the waveguide achieves side-mode suppression and a Q factor of $\sim 10^8$. To date, ring

resonators have been exploited in many formats such as microdroplets [25], microknots [26], and microcapillaries [27], providing excellent optical feedback for low-threshold lasing.

B. Optofluidic Prisms

How to achieve accurate alignment among multiple optical components is one of the main challenges when designing an optofluidic system. The use of an optofluidic prism to manipulate the light path would greatly alleviate such an integration issue. To this end, a configurable optofluidic prism was reported in Ref. [28]. By converging three laminar flow streams in a triangular chamber, the apex angle of the prism can be adjusted by altering the flow rates of the streams. Thus, one can steer the optical path in-plane due to refraction of light at the interface of two fluids. Further explorations on optofluidic prisms focus on system rotatability and robustness of optical scanning. Zappe's group developed a 360° rotatable optofluidic prism, which enabled rotational beam scanning in 16 discrete steps [Figs. 1(c) and 1(d)] [29]. A cylindrical fluidic chamber comprising two immiscible liquids is wrapped with flexible polymeric foils. Segmented electrodes are embedded in the foils. Upon applying variable voltages over the electrodes, the local contact angle of the liquid interface can be changed due to the electro-wetting effect. In this device, the total number of beam positions is determined by the number of electrodes, meaning that more meticulous beam rotation can be achieved by using more discrete electrodes.

C. Optofluidic Switches

As an important part of an optofluidic imaging system, optical switches can modify light path and intensity [30,31]. A 2 × 2 optofluidic switch based on total internal reflection was proposed by Campbell *et al.* [31]. The device was fabricated using soft lithography, consisting of two distinct layers, which are separated by a thin PDMS membrane with a low Young's modulus [Fig. 2(a)]. The upper layer is a fluidic layer containing a mirror channel with two inlets (one for a low-RI medium and the other for a high-RI medium), and the lower layer is a control layer containing five pneumatic valves. These valves are used to control the exchange of sample media in the mirror channel. Upon illumination, the light beam can be transmitted or reflected by tuning the RI of the medium in the mirror channel. Huang's group developed an acoustic-driven optofluidic switch [32], which consists of a microfluidic channel that is sandwiched between air-filled cavities in PDMS. Deionized water (RI of 1.33) and $CaCl_2$ solution (RI of 1.42) are introduced into the main channel. When the piezoelectric transducer is turned off, the incident laser beam is reflected at the interface between the PDMS (RI of 1.41) and deionized water [Fig. 2(b)]. On the contrary, when the transducer is turned on, the oscillating cavities mix the two media, and the incident laser beam is transmitted through the microchannel since the RI of the mixed solution is close to that of PDMS [Fig. 2(c)].

D. Optofluidic Lenses

As an essential component in optofluidic systems, lenses are used to adjust the light intensity, beam profile, and light propagation direction of the optical systems [33,34]. Optofluidic lenses can be categorized into in-plane and out-of-plane lenses, depending on the light propagation direction [12,19]. Yu *et al.* presented a hydrodynamic out-of-plane optofluidic lens consisting of two layers; this was fabricated by soft lithography and is shown in Fig. 2(d) [35]. The lower layer contains a circular PDMS aspherical surface, which can effectively compensate for spherical aberration and improve the optical quality. The upper layer, however, is a PDMS elastic membrane. By controlling the injection pressure in the microchannel, the surface contour of the upper layer can be changed, and the focal length of the lens is adjusted dynamically. Other approaches such as using stimuli-responsive hydrogels [36], electrical tuning [37], and changing a medium's refractive index [38] have also been exploited to adjust the focal length of out-of-plane optofluidic lenses.

Since the fabrication process of out-of-plane lenses is relatively complex and the structures should be well aligned, their applications in optofluidic systems are limited in many cases [12,34]. In-plane optofluidic lenses, on the other hand, offer

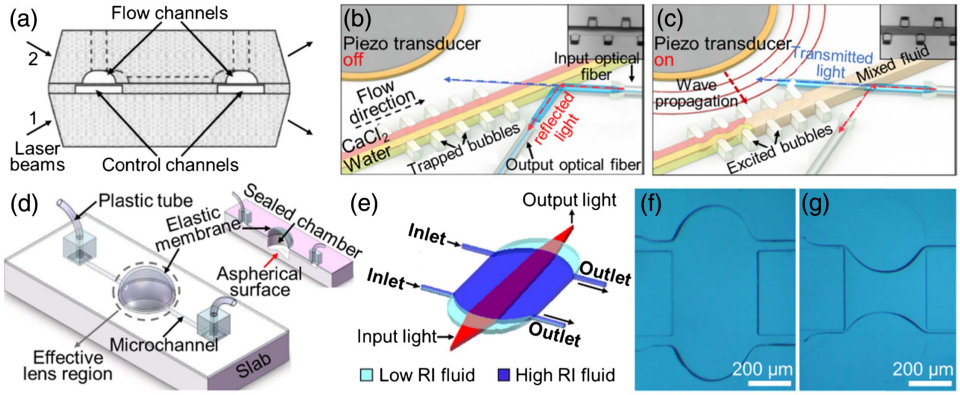

Fig. 2. (a) Schematic of a three-layer optofluidic switch with four optical facets. The arrows show the directions of both incident and reflected/transmitted laser beams. (b), (c) Working mechanism of an acoustic-driven optofluidic switch (b) without and (c) with acoustic excitation. (d) Schematic of a liquid-filled out-of-plane lens. The inset illustrates the cross section of the device. (e) Schematic of an in-plane optofluidic lens. The high-RI fluid medium forms a biconvex microlens that focuses the incident light. (f), (g) Experimental images on (f) the biconvex microlens and (g) the biconcave microlens. (a) Reproduced with permission [31], Copyright 2004, American Institute of Physics. (b), (c) Reproduced with permission [32], Copyright 2012, American Institute of Physics. (d) Reproduced with permission [35], Copyright 2010, Optical Society of America. (e)–(g) Reproduced with permission [41], Copyright 2017, Optical Society of America.

more compatibility. The geometry of an in-plane optofluidic lens can be changed to adjust its focal length by pneumatic tuning [39], thermal driving [40], etc. Fang *et al.* presented a hydrodynamic optofluidic lens [41] in which silicone oil and $CaCl_2$ solution can be injected into an expanded chamber and used as the lens cladding and core layers [Fig. 2(e)], respectively; the refractive index of the cladding streams is matched with that of the device's material to avoid light scattering. By tuning the flow rates of the streams, the lens geometry can be changed into the biconvex [Fig. 2(f)], plano, or biconcave format [Fig. 2(g)]. The incident light can therefore be converged, collimated, or diverged accordingly.

Interestingly, it has also been reported that biological materials such as cyanobacteria [42], diatoms [43], red blood cells (RBCs) [44], and spider silks [45] also show the capability to focus light into a confined region, acting as bio-microlenses. Miccio *et al.* demonstrated using an RBC as an adaptive optofluidic microlens to perform real-time, fine-resolution measurement on chip [44]. Li *et al.* trapped living yeast and human cells of spherical or disc shapes on a fiber probe to confine the excitation light to a sub-wavelength region and achieve fluorescence enhancement [46].

As described above, optofluidic components have shown great potential with respect to various on-chip optical processes. It is envisioned that in the near future, all optical components, as well as full functionalities, can be integrated into a single chip. In terms of microscale imaging in an integrated platform, such optofluidic components and their combinations have to address several critical challenges. First, unlike solid-state optical elements, the physical properties of a liquid medium are prone to be unstable and temperature-dependent, and any disturbance such as heat dissipation would compromise the device's performance. Flow control is another concern whenever a continuous liquid supply is required. In particular, most structural materials in microfluidic systems have refractive indices very close to the RI range of the liquids, which hampers the capability to tightly focus a light beam with a high NA. In other words, it is extremely difficult to achieve imaging with high resolution and high signal-to-noise ratios when using optofluidic components. Therefore, the most recent research efforts on optofluidic imaging have generally taken a new approach: eschewing optofluidic elements and focusing on methods for image capture. These works will be discussed in the next section.

3. OPTOFLUIDIC IMAGING METHODS

As mentioned above, one can easily observe that the optofluidic components still follow the original definition of optofluidics as using fluids to manipulate optical mechanics. Yet from the perspective of an integrated imaging system, the assembly of individual components and the use of novel image-capturing methods form other important aspects of an optofluidic imaging system. Such works are no longer constrained by the original definition of optofluidics. In fact, as illustrated by the authors in the Introduction section, either when there is synergy between the optical and fluidic domains of the system, or when advanced optical/photonic methods are used to concretize enhanced deployment, reliability, accuracy, and throughput of the system, especially in the on-chip aspect, can it be defined as an optofluidic system. In this section, we will demonstrate recent activities on integrated optofluidic imaging systems in two categories, namely, lens-based and lens-free schemes.

A. Lens-Based Optofluidic Imaging

Optical microscopy has revolutionized bio-imaging and is the most investigated method to characterize biomolecules on-chip. Thriving efforts have demonstrated a variety of modalities applied in optofluidics, including bright-field and fluorescence microscopy [47–49], phase-contrast microscopy [50], confocal microscopy [51], differential interference contrast microscopy [52], etc. Due to the lens structure in the imaging system, such techniques are also referred to as lens-based imaging.

However, in terms of biomolecular imaging, lens-based microscopy techniques have encountered three major obstacles. (1) Bulky instruments. The bulky nature of conventional optical microscopes restricts them from being widely integrated with compact on-chip microfluidic/optofluidic devices. Miniaturizing the whole microscopic system into a chip-size device still has a long way to go. Laborious operation and high cost are also negative factors, which compel the use of lens-based imaging mainly in a laboratory environment by well-trained personnel. (2) Diffraction-limited resolution. The wave nature of light imposes a limit on the resolution in conventional optical microscopy with which one can resolve features of around half of the wavelength of illumination, λ. This limitation on resolution hinders the application of lens-based microscopy in subcellular or biomolecular imaging, meaning nanofeatures such as exosomes [53], proteins, and DNAs cannot be clearly resolved. However, these objects are the keystone to map molecular dynamics in terms of modern pathology and physiology. Current studies are conducted as either sensing rather than imaging [54,55] or interrogating a population of interest rather than a comprehensive characterization of morphology at the single molecular level. (3) Trade-off between field of view (FOV) and resolution of the imaging system. To achieve simultaneous imaging of multiple sections on a chip, an image sensor with a large FOV is required, which typically means that a lens with a low NA is also used, corresponding to a low spatial resolution. Hence, the demand for high spatial resolution contradicts the total throughput of the optical system. Recent innovations on advanced computational methods have made it possible to retrieve both high-resolution and wide-field images [56,57].

Although super-resolution strategies such as stimulated emission depletion microscopy [58], fluorescence photoactivation localization microscopy [59], and stochastic optical reconstruction microscopy [60] have achieved three-dimensional (3D) imaging with resolution better than a few tens of nanometers, none has yet been incorporated within an optofluidic system. As an alternative approach, some researchers focus on providing richer information and higher throughput while preserving the current resolution and throughput. One remarkable example is light-sheet fluorescence microscopy (LSFM), also referred to as selective plane illumination microscopy. Using a laser light sheet as planar illumination, LSFM provides higher acquisition speed over an extended 3D sample than conventional point-illumination microscopy. Besides, with high sectioning capability (compared with confocal microscopy), a large FOV, and rapid scanning speed (compared with epifluorescence microscopy), as well as reduced

photobleaching, LSFM has proven to be a strong 3D imaging technique [61]. Bruns *et al.* first proposed combining LSFM with fluidic devices [62]. Regmi *et al.* presented a PDMS chip to perform sample delivery, where the chip was coupled to a customized light-sheet microscope [63]. Later, efforts have been dedicated to integrating both sample delivery functions and optical components into a single chip. Deschout *et al.* proposed a light-sheet generation unit on chip [Fig. 3(a)] [64], while Paiè *et al.* achieved full integration of illumination and sample scanning [Fig. 3(b)] [65]. The light sheet, generated with an optofluidic cylindrical lens, was focused on a microfluidic channel and allowed continuous imaging of cell spheroids [66]. Attempts to use microfabricated components for planar illumination and fluorescent light collection have also been demonstrated by Zagato *et al.* [67] and Meddens *et al.* [68]. This implies the possibility to achieve super-resolution and single-object imaging on a more compact and portable device in the near future. Bianco *et al.* proposed an alternative method to employ the lens-based approach on-chip [69]. As shown in Fig. 3(c), a diffraction grating is fabricated on the chip surface, which allows the extraction of the reference wavefront directly from the object beam, thus enabling the formation of hologram fringes. Thus, it can be used to produce off-axis holograms from single-beam illumination. The holograms are recorded with a CCD camera through an objective lens, providing information of the sample.

B. Lens-Free Optofluidic Imaging

Advanced microelectronics and emerging computational microscopy techniques have provided another scheme to bypass the various limitations of conventional optical microscopy. In a lens-free imaging setup, an image sensor (CMOS/CCD) is typically placed beneath the sample and used to record light transmission pixel by pixel. By abandoning lens components, such a lens-free (or lensless) scheme offers great possibilities to provide a compact and non-diffraction-limited imaging technique with a large FOV and shows great flexibility on the integration format. In the last decade, multiple lens-free on-chip microscope modi have been proposed to perform imaging on microorganisms [70] and cells [71], showing exciting breakthroughs in point-of-care applications.

1. Lens-Free Optofluidic Microscope

A lens-free, on-chip microscope termed an "optofluidic microscope (OFM)" was reported by Yang's group in 2008. Different from early imaging methods by simply placing a specimen on an image sensor, the OFM employs clever modification to achieve much better resolution than the pixel size of the image sensor. Using a nanofabrication process, a thin metal layer with two aperture lines is embedded in the optofluidic device above a CMOS sensor. Each aperture (<1 μm) is aligned on top of one CMOS pixel, forming two parallel lines running across the CMOS sensor with a slight diagonal from the channel direction [Fig. 4(a)] [16]. Upon illumination, the CMOS pixels collect light transmission signals when the specimen translates over the apertures. Therefore, the resolution of the imaging system is no longer governed by the pixel size of the CMOS sensor, which is normally larger than 1 μm (such as the ones used in smartphone cameras), but is determined by the aperture size. The latter can be easily shrunk down to a few tens of nanometers with modern nanofabrication methods [72]. In addition, the CMOS sensor can be replaced with a CCD imager with a large pixel size, high pixel counts, and low optical noise for better image quality [73]. The OFM was first used to image the nematode *Caenorhabditis elegans*, as shown in Fig. 4(b). Later, with DC electrokinetics and innovative microfluidic designs, spherical/ellipsoidal samples such as pollen spores, *Chlamydomonas*, and

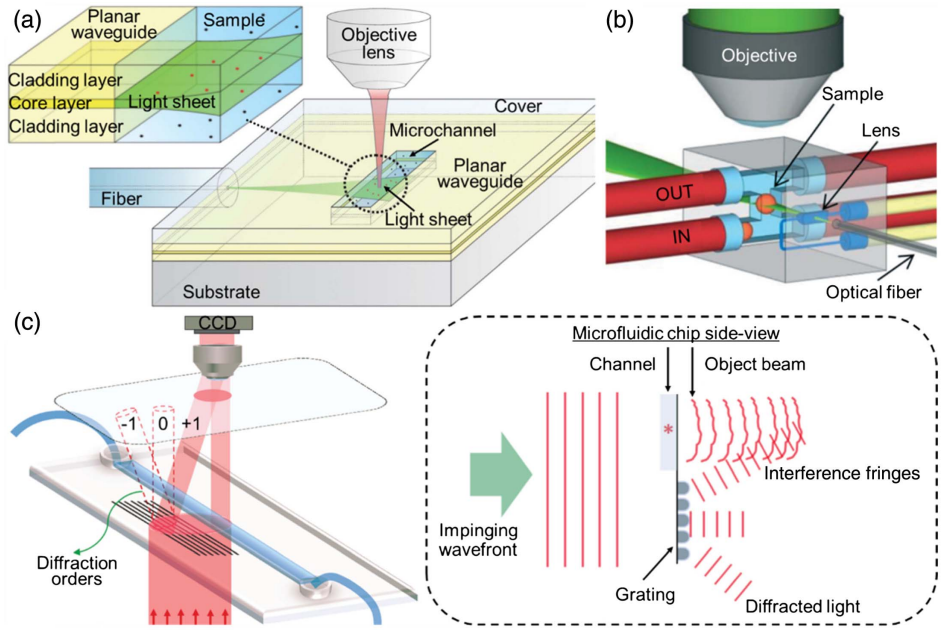

Fig. 3. (a) Planar waveguide integrated on-chip to create a light sheet directly on the sample. (b) Optofluidic lens integrated on-chip to focus a light sheet at the center of a fluidic channel, where multiple samples are automatically scanned and reconstructed in 3D. (c) Working principle of single-beam interferometry. (a) Reproduced with permission [64], Copyright 2014, Royal Society of Chemistry. (b) Reproduced with permission [65], Copyright 2016, Royal Society of Chemistry. (c) Reproduced with permission [69], Copyright 2017, Nature Publishing Group.

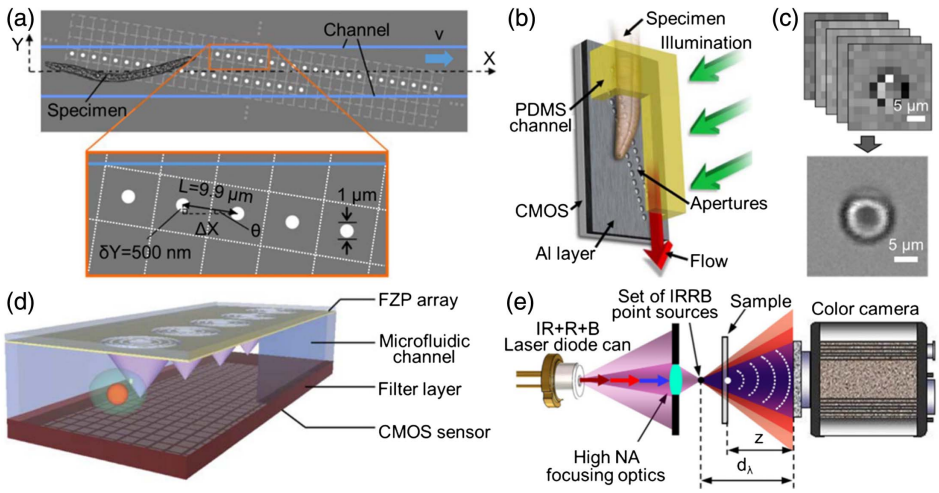

Fig. 4. Examples of an OFM. (a) Schematic of an OFM device (top view). The OFM apertures (white circles) are defined on a 2D CMOS image sensor (light gray dashed grid) coated with Al (gray) and span across the whole microfluidic channel (blue lines). (b) Upright operation mode of the OFM device. (c) Low-resolution sequence of a single RBC to a high-resolution image. (d) Schematics of an FZP-based fluorescence optofluidic microscope. A sample flows in the microfluidic channel on top of the image sensor. The FZP array creates an array of foci inside the channel. (e) Layout for MISHELF microscopy with detuned illumination/detection using IRRB/RGB multiplexing. (a), (b) Reproduced with permission [16], Copyright 2008, National Academy of Sciences of the USA. (c) Reproduced with permission [71], Copyright 2011, PLOS. (d) Reproduced with permission [76], Copyright 2011, Royal Society of Chemistry. (e) Reproduced with permission [77], Copyright 2017, Nature Publishing Group.

Giardia lamblia trophozoites and cysts were successfully imaged at a resolution of 800 nm [16,74].

In 2010, a new derivative was proposed where multiframe super-resolution algorithms were employed in a new OFM scheme to capture and reconstruct high-resolution images [75]. By rearranging a sequence of 40–50 low-resolution raw images into a high-resolution matrix, the translation characters (e.g., motion vectors) of a specimen in a laminar flow would be determined and substituted into the imaging algorithm, thus allowing one to retrieve images of the sample flowing under a low-speed pressure-driven condition. Referred to as the sub-pixel resolving OFM, this novel OFM technique does not require a metal mask and sub-micrometer apertures, and achieves a higher acquisition rate than the aperture-based OFM, with a maximum frame rate of 75,000 frames/s at an FOV of 50 mm [Fig. 4(c)] [71]. Additionally, a Fresnel zone plate (FZP) provides another variation of the OFM. FZP arrays act as high-NA microscope objective lenses and focus illumination light into a nanoscale [Fig. 4(d)] [76]. Compared with aperture-based OFM, which requires placing metal-coated CMOS adjacent to the biological sample, the FZP scheme enables reusing the image sensor after each test and enhances sensitivity by isolating heat transfer. A new compact, field-portable, lens-free microscope prototype, namely, MISHELF (multi-illumination single-holographic-exposure lensless Fresnel), was proposed in 2017 [shown in Fig. 4(e)] [77]. Such a device uses RGB lasers as three illumination sources, which are focused into a set of three slightly laterally and axially shifted point sources below the sample. The resulting multiplexed Fresnel patterns are extracted and fused based on a convergence algorithm for twin image minimization and noise reduction.

2. Lens-Free Tomographic Microscope

A highly compact and portable tomographic microscopy system pioneered by Ozcan's group was reported in 2011 [78]. In a typical lens-free on-chip microscope, a semi-transparent sample is sandwiched between a partially coherent light source (distance $Z_1 > 2$–3 cm) and an image sensor (distance $Z_2 < 1$ mm), casting an in-line hologram [Fig. 5(a)]. Single perspective holography provides individual 3D sectioning information, and a whole tomographic reconstruction is feasible while using illumination from different angles to capture a sequence of holograms of the same object. Moreover, fiber-coupled light-emitting diodes (LEDs) working as light sources can be individually controlled to create holograms of objects on a CMOS sensor, as shown in Fig. 5(b). The recorded lens-free holograms are used to generate transmission images with resolution better than 1 μm over an FOV of 24 mm, i.e., ~50 times larger than that with a conventional microscope with similar resolution [79].

Color imaging is vital in many biomedical applications since it provides additional information and contrast of the sample. However, the coherent illumination of the lens-free tomographic microscope requires monochromatic light, resulting in monochrome images. A pseudo-colored scheme was demonstrated in 2014 by using a computational method to digitally colorize human carcinoma cells according to statistical intensity mapping; the results obtained were comparable to those with a traditional lens-based color microscope [80]. Multiple holograms generated at different illumination wavelengths are also utilized to synthesize a color image (e.g., RGB space), although accompanied by undesirable "rainbow" artifacts and triple data acquisition time [81]. A modification called the YUV method can be used to average the color information in lower resolution in the UV channels and then convert it to the RGB space, thereby mitigating the "rainbow" artifacts. Meanwhile, the Y channel represents brightness information in pixel super-resolution, and is merged with the UV channels into a finalized image [Figs. 5(c)–5(e)] [82].

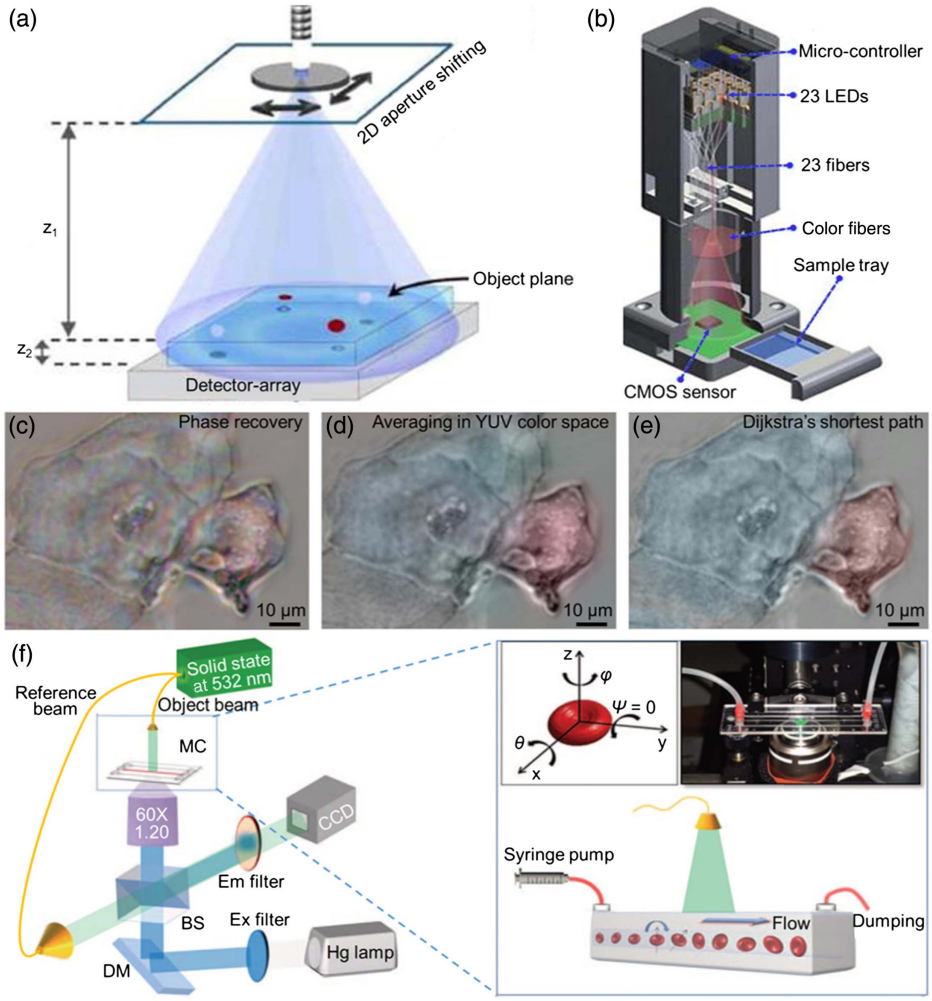

Fig. 5. Different lens-free tomographic microscopes. (a) Schematic of a tomographic microscope device integrated with a shifting aperture. (b) An array of static light sources, e.g., fiber-coupled LEDs are used to create lens-free holograms. (c) "Rainbow" artifact in the reconstructed holograms. (d) Result of the YUV colorization method. (e) An image of the same sample with a 20× objective (NA = 0.5) microscope. (f) Schematic of tomographic phase microscopy. Cell tumbling behavior in a microfluidic channel is used to analyze the holograms. (a) Reproduced with permission [78], Copyright 2011, Optical Society of America. (b) Reproduced with permission [79], Copyright 2011, Royal Society of Chemistry. (c)–(e) Reproduced with permission [82], Copyright 2013, Optical Society of America. (f) Reproduced with permission [85], Copyright 2017, Nature Publishing Group.

More recently, Zhang *et al.* presented a multiplexed hologram by using three illumination wavelengths simultaneously to generate chromatic high-resolution images on a smartphone [83].

Utilizing tomographic imaging is challenging when a sample is transported in a continuous flow, given that it requires a complex setup to rotate the sample/light source and examine the sample in multiple directions. Ferraro's group first demonstrated a continuous-flow cytotomography on an optofluidic platform. As presented in Fig. 5(f), by exploiting cell tumbling behavior using fluidic dynamics [84], different angular positions of the cells are recorded while they are rolling in a microfluidic channel. Such an acquired hologram is transformed to reconstruct the complex wavefield (both amplitude and phase) diffracted by the cells from every single coordinate [85]. This approach allows cytotomography and complete morphologic study via self-rotation of cells at a speed of hundreds of cells per minute, without requiring any mechanical/optoelectronic control. Such a format greatly reduces the complexity of the experimental setup, showing possibilities of a higher level of integration between optofluidics and lens-free tomography for morphology study and further disease diagnosis.

4. AUXILIARY MODULES OF AN OPTOFLUIDIC IMAGING SYSTEM

Regarding applications of bio-imaging, one must realize that it concerns not only biology and fluid deployment and optical microscopy interrogation, but also image acquisition methods and processing algorithms. In general, there are two technical knots that tie up current optofluidic imaging applications: (1) nanoscale on-chip manipulation of bio-samples and (2) fast data acquisition/processing rate. The former represents sample-handling methods, showing whether the imaged object could be shrunk down to the subcellular level, whereas the latter normally determines the

throughput and data details obtained from an imaging system. In a fully integrated system, optofluidic components and imaging methods (mentioned in Sections 2 and 3) comprise the core module, whereas on-chip sample manipulation and data acquisition/processing methods constitute the auxiliary modules. In this section, we will briefly describe the auxiliary modules and their challenges in next-generation optofluidic imaging technologies.

Biologists today are eager to establish a map of biomolecular interactions inside our body. Although current bio-imaging studies are mostly established on a population of interest, rather than studies on individual biomolecules, imaging on a single-molecule basis can provide us with information on morphology statistics and physicochemical properties, as well as molecular dynamics. However, collecting nanometer-size target molecules from a complex sample (e.g., serum) is highly challenging. Besides, the need to position, focus on, and image each individual molecule actually hampers imaging in practice. Optical methods for sample manipulation, such as optical stretcher and optical tweezer, are mature techniques, which can realize on-chip cell sorting, trapping, and even 3D rotation [86,87]. However, when the imaging features (e.g., extracellular vesicles, proteins) are in the nanometer range, optical methods are no longer able to manipulate them in the solution. Although some novel optofluidic designs have achieved separating sub-100 nm gold particles [88], it remains impossible to differentiate biomolecules from a medium, since the interaction between the biomolecules and the external field (e.g., optical/electrophoretic/acoustical) is too weak and could be buried in background noise. New techniques on sample handling have been published. Wunsch *et al.*, for instance, utilized nano deterministic lateral displacement pillar arrays to perform on-chip sorting and quantification of exosomes down to 20 nm [89]. Han's group presented nanofilter arrays synergized with an electric field to separate protein aggregates [90]. These studies with structural confinement are inspiring and will possibly benefit future on-chip nanoscale sample sorting and manipulation, to differentiate specific biomolecules for further imaging operations.

To illustrate data acquisition/processing methods, on should note the concept of "data momentum," i.e., a figure of merit defined as an outcome of the measured information content ("data mass") and the throughput of the measurement ("data velocity"). Often as researchers desire more comprehensive measurement content ("mass") in a single shot, it comes at the cost of a lower throughput ("velocity") [91]. One of the most exciting innovations in ultrafast imaging, namely, optical time-stretch imaging, has been proven to enable continuous operation at a time resolution (time per frame) of a sub-microsecond [92] or even a sub-nanosecond [93], which exceeds that of any classical imaging systems. Utilizing this method with microfluidic systems also shows intriguing compatibilities [94,95]. The core concept of optical time-stretch imaging is to retrieve spatial information from the "time-stretch" spectrum in the one-dimensional (1D) temporal data stream. The entire process involves two mapping steps: frequency-to-space encoding and frequency-to-time decoding, as illustrated in Fig. 6(a). The whole spatial coordinates can be decomposed from multiple frequency components after an optical disperser (e.g., a diffraction grating or a prism), resulting in one-to-one frequency-to-space mapping. Thus, the total spectral bandwidth of the laser pulse determines the imaging FOV. The spatial encoded spectrum is temporally stretched into a 1D temporal data stream, namely, a process known as dispersive Fourier transformation. This process extensively reduces the data storage size and achieves real-time digitalization in a single

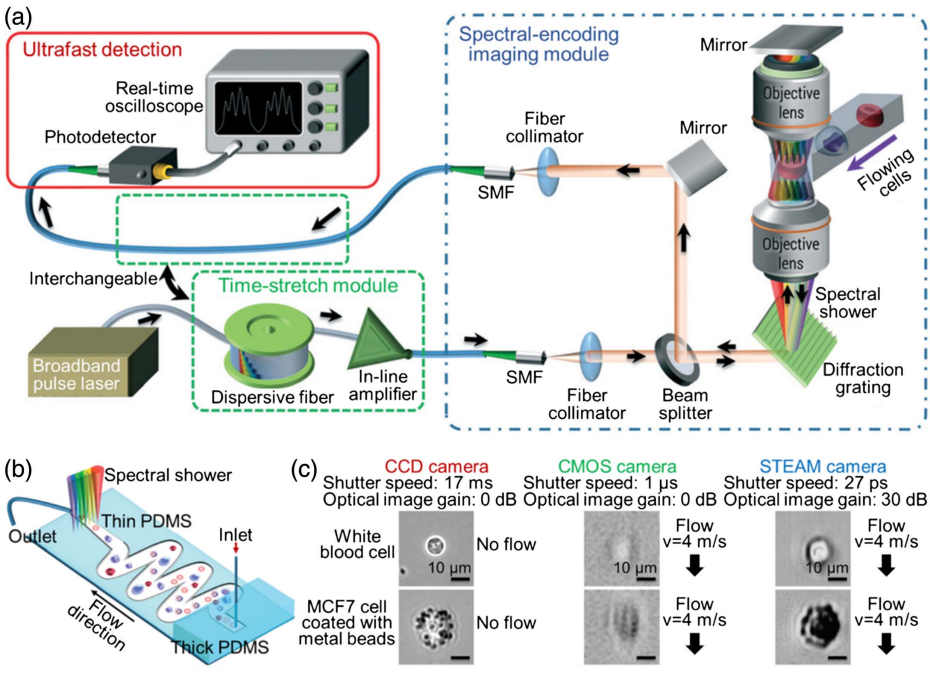

Fig. 6. (a) Schematics of optofluidic time-stretch imaging. (b) Microfluidic channel design used for time-stretch imaging, which relies on an inertial focusing scheme to constrain the position of flowing cells into a straight stream in the imaging region. (c) White blood cell and stained MCF7 cell images captured with CCD, CMOS, and time-stretch cameras. The scale bars represent 10 μm. (a), (b) Reproduced with permission [91], Copyright 2016, Royal Society of Chemistry. (c) Reproduced with permission [95], Copyright 2012, National Academy of Sciences of the USA.

pulse, allowing continuous broadband spectral retrieval by simply using a high-speed photodetector and a digitizer [91]. Given its ability in ultrafast imaging, the optical time-stretch method was recently employed in an optofluidic platform for single-cell imaging. Using a serpentine microfluidic channel configuration, imaging of cancer cells and blood cells was realized at a high flow speed of ∼10 m/s, showing intriguing compatibility in an optofluidic system and a conventional microscope setup [Fig. 6(b)]. Nevertheless, high-speed CMOS/CCD cameras still suffer from image blurring due to the motion of the sample while capturing ultrafast subjects with high resolution [Fig. 6(c)] [95]. Wong *et al.* demonstrated the use of asymmetric-detection time-stretch optical microscopy in cell counting, presenting a data rate of up to ∼100,000 cells/s, which is faster than that of any other existing flow cytometer [96]. Another morphological analysis method, which was proposed by Ugawa *et al.*, achieved a resolution of 780 nm with a throughput of 10,000 particles per second, better than those of previous imaging-based particle analyzers [97]. To further explore the capability of time-stretch imaging techniques for optofluidic analysis, multimodalities to identify molecular signatures and search for underexploited biophysical parameters are the obvious trends.

5. CONCLUSION

We hope this review has made it clear that the integration of optical elements with microfluidic platforms can advantageously contribute to bio-imaging applications and that such integration is key to improvement of the performance of an optical imaging system, including its resolution and throughput. To help the broad audience construct their comprehension of optofluidic imaging, we first reviewed the basic composition of an optofluidic system, focusing on four classes of components, namely, optofluidic lasers, prisms, switches, and lenses. These elements have shown great potential in various on-chip optical processes but several challenges need to be addressed—for example, disturbance of optical properties due to instability of the liquid medium, difficulty of flow control, and similar refractive indices of the liquid and most structural materials of microfluidic systems.

We consecutively discussed the imaging methods used for optofluidic bio-imaging applications in two major schemes, namely, lens-based and lens-free imaging. A lens-based system is generally diffraction-limited, and high resolution comes with a small FOV. Different groups have proposed using LSFM to overcome the difficulties mentioned above. On the other hand, by abandoning the lens components, lens-free imaging systems can achieve a large FOV and non-diffraction-limited resolution, and show greater flexibility on an integration format. Considering the booming point-of-care and *in vitro* diagnosis industries, lens-free optofluidic imaging systems are very promising to incorporate with advanced consumer electronics and revolutionize today's medical and clinical systems.

Nowadays, there is a significant demand for high-resolution and high-throughput imaging techniques to reveal molecular dynamics and intracellular communications. In an integrated optofluidic imaging system, not only are optofluidic components and imaging methods necessary, but on-chip manipulation of nanometer-size biological samples and advanced data acquisition/processing methods also play important roles. New techniques for sample handling were discussed, followed by introduction of recent fast data acquisition methods—for example, time-stretch optical microscopy, which can achieve ultrafast single-cell imaging, and was also employed in optofluidic platforms.

Summarizing, we believe that the integration of optical components with microfluidic systems presents key advantages for many large-scale biological studies at the individual cell and molecule levels, and is of benefit to automated sample screening and imaging. Overall, optofluidic technologies have largely demonstrated potential to dramatically improve many aspects of biological research by providing superior performance when compared with classical protocols. Looking forward to the forthcoming decade, we are convinced that technical emergences in the aspect of optofluidic bio-imaging would be displayed at multiple levels: (1) nanoscale molecular imaging in leading-edge studies of microvesicles, protein expression, and DNA decoding; (2) improved degree of integration for bioassays, specifically combining consumer electronics in point-of-care applications; and (3) ultrafast imaging in molecular screening and analysis in a clinical concern. The ongoing transition of bio-imaging applications from an observation-based discipline to a mechanism-based science suggests that systems capable of imaging samples with high resolution and high data acquisition speed in a well-defined spatiotemporal manner will become invaluable tools. Optofluidic imaging techniques will play a prominent role in this endeavor. We hope that this review will serve as a compilation to outline the developing route in optofluidic imaging and present its potent role in biology/medicine/pathology studies in the future.

Funding. National Natural Science Foundation of China (NSFC) (61805271); Guangdong Province Introduction of Innovative and Entrepreneurial Teams (2016ZT06D631); Shenzhen Science and Technology Innovation Commission (JCYJ20170818154035069).

REFERENCES

1. A. R. Kherlopian, T. Song, Q. Duan, M. A. Neimark, M. J. Po, J. K. Gohagan, and A. F. Laine, "A review of imaging techniques for systems biology," BMC Syst. Biol. **2**, 74 (2008).
2. K. König, "Multiphoton microscopy in life sciences," J. Microsc. **200**, 83–104 (2000).
3. F. Gaboriaud and Y. F. Dufrêne, "Atomic force microscopy of microbial cells: application to nanomechanical properties, surface forces and molecular recognition forces," Colloids Surf. B **54**, 10–19 (2007).
4. M. A. Hamburg and F. S. Collins, "The path to personalized medicine," N. Engl. J. Med. **363**, 301–304 (2010).
5. K.-H. Jung and K.-H. Lee, "Molecular imaging in the era of personalized medicine," J. Pathol. Transl. Med. **49**, 5–12 (2015).
6. P. Minzioni, R. Osellame, C. Sada, S. Zhao, F. Omenetto, K. B. Gylfason, T. Haraldsson, Y. Zhang, A. Ozcan, A. Wax, F. Mugele, H. Schmidt, G. Testa, R. Bernini, J. Guck, C. Liberale, K. Berg-Sørensen, J. Chen, M. Pollnau, S. Xiong, A.-Q. Liu, C.-C. Shiue, S.-K. Fan, D. Erickson, and D. Sinton, "Roadmap for optofluidics," J. Opt. **19**, 093003 (2017).
7. X. Mao, S.-C. S. Lin, C. Dong, and T. J. Huang, "Single-layer planar on-chip flow cytometer using microfluidic drifting based three-dimensional (3D) hydrodynamic focusing," Lab Chip **9**, 1583–1589 (2009).
8. X. Mao, A. A. Nawaz, S.-C. S. Lin, M. I. Lapsley, Y. Zhao, J. P. McCoy, W. S. El-Deiry, and T. J. Huang, "An integrated, multiparametric flow cytometry chip using 'microfluidic drifting' based three-dimensional hydrodynamic focusing," Biomicrofluidics **6**, 024113 (2012).

9. M. I. Lapsley, I.-K. Chiang, Y. B. Zheng, X. Ding, X. Mao, and T. J. Huang, "A single-layer, planar, optofluidic Mach–Zehnder interferometer for label-free detection," Lab Chip **11**, 1795–1800 (2011).
10. J. S. Mak, S. A. Rutledge, R. M. Abu-Ghazalah, F. Eftekhari, J. Irizar, N. C. Tam, G. Zheng, and A. S. Helmy, "Recent developments in optofluidic-assisted Raman spectroscopy," Prog. Quant. Electron. **37**, 1–50 (2013).
11. X. Fan and S. H. Yun, "The potential of optofluidic biolasers," Nat. Methods **11**, 141–147 (2014).
12. N.-T. Nguyen, "Micro-optofluidic lenses: a review," Biomicrofluidics **4**, 031501 (2010).
13. X. Fan, I. M. White, S. I. Shopova, H. Zhu, J. D. Suter, and Y. Sun, "Sensitive optical biosensors for unlabeled targets: a review," Anal. Chim. Acta **620**, 8–26 (2008).
14. N.-T. Huang, H.-L. Zhang, M.-T. Chung, J. H. Seo, and K. Kurabayashi, "Recent advancements in optofluidics-based single-cell analysis: optical on-chip cellular manipulation, treatment, and property detection," Lab Chip **14**, 1230–1245 (2014).
15. C. Monat, P. Domachuck, and B. J. Eggleton, "Integrated optofluidics: a new river of light," Nat. Photonics **1**, 106–114 (2007).
16. X. Cui, L. M. Lee, X. Heng, W. Zhong, P. W. Sternberg, D. Psaltis, and C. Yang, "Lensless high-resolution on-chip optofluidic microscopes for *Caenorhabditis elegans* and cell imaging," Proc. Natl. Acad. Sci. USA **105**, 10670–10675 (2008).
17. D. Erickson, D. Sinton, and D. Psaltis, "Optofluidics for energy applications," Nat. Photonics **5**, 583–590 (2011).
18. T. Yang, F. Bragheri, and P. Minzioni, "A comprehensive review of optical stretcher for cell mechanical characterization at single-cell level," Micromachines **7**, 90 (2016).
19. C. Song and S. H. Tan, "A perspective on the rise of optofluidics and the future," Micromachines **8**, 152 (2017).
20. Y. Zhao, Z. S. Stratton, F. Guo, M. I. Lapsley, C. Y. Chan, S.-C. S. Lin, and T. J. Huang, "Optofluidic imaging: now and beyond," Lab Chip **13**, 17–24 (2013).
21. D. V. Vezenov, B. T. Mayers, R. S. Conroy, G. M. Whitesides, P. T. Snee, Y. Chan, D. G. Nocera, and M. G. Bawendi, "A low-threshold, high-efficiency microfluidic waveguide laser," J. Am. Chem. Soc. **127**, 8952–8953 (2005).
22. W. Song, A. E. Vasdekis, Z. Li, and D. Psaltis, "Optofluidic evanescent dye laser based on a distributed feedback circular grating," Appl. Phys. Lett. **94**, 161110 (2009).
23. X. Fan and I. M. White, "Optofluidic microsystems for chemical and biological analysis," Nat. Photonics **5**, 591–597 (2011).
24. W. Lee, H. Li, J. D. Suter, K. Reddy, Y. Sun, and X. Fan, "Tunable single mode lasing from an on-chip optofluidic ring resonator laser," Appl. Phys. Lett. **98**, 061103 (2011).
25. S. K. Tang, Z. Li, A. R. Abate, J. J. Agresti, D. A. Weitz, D. Psaltis, and G. M. Whitesides, "A multi-color fast-switching microfluidic droplet dye laser," Lab Chip **9**, 2767–2771 (2009).
26. X. Jiang, Q. Song, L. Xu, J. Fu, and L. Tong, "Microfiber knot dye laser based on the evanescent-wave-coupled gain," Appl. Phys. Lett. **90**, 233501 (2007).
27. S. I. Shopova, H. Zhou, X. Fan, and P. Zhang, "Optofluidic ring resonator based dye laser," Appl. Phys. Lett. **90**, 221101 (2007).
28. S. Xiong, A. Liu, L. Chin, and Y. Yang, "An optofluidic prism tuned by two laminar flows," Lab Chip **11**, 1864–1869 (2011).
29. D. Kopp, L. Lehmann, and H. Zappe, "Optofluidic laser scanner based on a rotating liquid prism," Appl. Opt. **55**, 2136–2142 (2016).
30. L. Pang, H. M. Chen, L. M. Freeman, and Y. Fainman, "Optofluidic devices and applications in photonics, sensing and imaging," Lab Chip **12**, 3543–3551 (2012).
31. K. Campbell, A. Groisman, U. Levy, L. Pang, S. Mookherjea, D. Psaltis, and Y. Fainman, "A microfluidic 2 × 2 optical switch," Appl. Phys. Lett. **85**, 6119–6121 (2004).
32. P.-H. Huang, M. I. Lapsley, D. Ahmed, Y. Chen, L. Wang, and T. J. Huang, "A single-layer, planar, optofluidic switch powered by acoustically driven, oscillating microbubbles," Appl. Phys. Lett. **101**, 141101 (2012).
33. Q. Chen, T. Li, Z. Li, J. Long, and X. Zhang, "Optofluidic tunable lenses for in-plane light manipulation," Micromachines **9**, 97 (2018).
34. X. Mao, S.-C. S. Lin, M. I. Lapsley, J. Shi, B. K. Juluri, and T. J. Huang, "Tunable liquid gradient refractive index (L-GRIN) lens with two degrees of freedom," Lab Chip **9**, 2050–2058 (2009).
35. H. Yu, G. Zhou, H. M. Leung, and F. S. Chau, "Tunable liquid-filled lens integrated with aspherical surface for spherical aberration compensation," Opt. Express **18**, 9945–9954 (2010).
36. L. Dong, A. K. Agarwal, D. J. Beebe, and H. Jiang, "Adaptive liquid microlenses activated by stimuli-responsive hydrogels," Nature **442**, 551–554 (2006).
37. K. Mishra, C. Murade, B. Carreel, I. Roghair, J. M. Oh, G. Manukyan, D. van den Ende, and F. Mugele, "Optofluidic lens with tunable focal length and asphericity," Sci. Rep. **4**, 6378 (2014).
38. Y. Hu, S. Rao, S. Wu, P. Wei, W. Qiu, D. Wu, B. Xu, J. Ni, L. Yang, J. Li, J. Chu, and K. Sugioka, "All-glass 3D optofluidic microchip with built-in tunable microlens fabricated by femtosecond laser-assisted etching," Adv. Opt. Mater. **6**, 1701299 (2018).
39. J. Shi, Z. Stratton, S.-C. S. Lin, H. Huang, and T. J. Huang, "Tunable optofluidic microlens through active pressure control of an air–liquid interface," Microfluid. Nanofluid. **9**, 313–318 (2010).
40. H. Liu, Y. Shi, L. Liang, L. Li, S. Guo, L. Yin, and Y. Yang, "A liquid thermal gradient refractive index lens and using it to trap single living cell in flowing environments," Lab Chip **17**, 1280–1286 (2017).
41. C. Fang, B. Dai, Q. Xu, R. Zhuo, Q. Wang, X. Wang, and D. Zhang, "Hydrodynamically reconfigurable optofluidic microlens with continuous shape tuning from biconvex to biconcave," Opt. Express **25**, 888–897 (2017).
42. N. Schuergers, T. Lenn, R. Kampmann, M. V. Meissner, T. Esteves, M. Temerinac-Ott, J. G. Korvink, A. R. Lowe, C. W. Mullineaux, and A. Wilde, "Cyanobacteria use micro-optics to sense light direction," ELife **5**, e12620 (2016).
43. E. De Tommasi, A. C. De Luca, L. Lavanga, P. Dardano, M. De Stefano, L. De Stefano, C. Langella, I. Rendina, K. Dholakia, and M. Mazilu, "Biologically enabled sub-diffractive focusing," Opt. Express **22**, 27214–27227 (2014).
44. L. Miccio, P. Memmolo, F. Merola, P. A. Netti, and P. Ferraro, "Red blood cell as an adaptive optofluidic microlens," Nat. Commun. **6**, 6502 (2015).
45. J. N. Monks, B. Yan, N. Hawkins, F. Vollrath, and Z. Wang, "Spider silk: mother nature's bio-superlens," Nano Lett. **16**, 5842–5845 (2016).
46. Y. Li, X. Liu, X. Yang, H. Lei, Y. Zhang, and B. Li, "Enhancing upconversion fluorescence with a natural bio-microlens," ACS Nano **11**, 10672–10680 (2017).
47. P. C. H. Li, L. de Camprieu, J. Cai, and M. Sangar, "Transport, retention and fluorescent measurement of single biological cells studied in microfluidic chips," Lab Chip **4**, 174–180 (2004).
48. D. Hess, A. Rane, A. J. deMello, and S. Stavrakis, "High-throughput, quantitative enzyme kinetic analysis in microdroplets using stroboscopic epifluorescence imaging," Anal. Chem. **87**, 4965–4972 (2015).
49. Y. Zeng, L. Jiang, W. Zheng, D. Li, S. Yao, and J. Y. Qu, "Quantitative imaging of mixing dynamics in microfluidic droplets using two-photon fluorescence lifetime imaging," Opt. Lett. **36**, 2236–2238 (2011).
50. M. Paturzo, A. Finizio, P. Memmolo, R. Puglisi, D. Balduzzi, A. Galli, and P. Ferraro, "Microscopy imaging and quantitative phase contrast mapping in turbid microfluidic channels by digital holography," Lab Chip **12**, 3073–3076 (2012).
51. M. Duocastella, G. Vicidomini, and A. Diaspro, "Simultaneous multiplane confocal microscopy using acoustic tunable lenses," Opt. Express **22**, 19293–19301 (2014).
52. C. Simonnet and A. Groisman, "Two-dimensional hydrodynamic focusing in a simple microfluidic device," Appl. Phys. Lett. **87**, 114104 (2005).
53. H. Shao, H. Im, C. M. Castro, X. Breakefield, R. Weissleder, and H. Lee, "New technologies for analysis of extracellular vesicles," Chem. Rev. **118**, 1917–1950 (2018).
54. Y. Sun and X. Fan, "Distinguishing DNA by analog-to-digital-like conversion by using optofluidic lasers," Angew. Chem. Int. Ed. **51**, 1236–1239 (2012).
55. Q. Chen, X. Zhang, Y. Sun, M. Ritt, S. Sivaramakrishnan, and X. Fan, "Highly sensitive fluorescent protein FRET detection using optofluidic lasers," Lab Chip **13**, 2679–2681 (2013).
56. G. Zheng, R. Horstmeyer, and C. Yang, "Wide-field, high-resolution Fourier ptychographic microscopy," Nat. Photonics **7**, 739–745 (2013).

57. L. Shao, P. Kner, E. H. Rego, and M. G. Gustafsson, "Super-resolution 3D microscopy of live whole cells using structured illumination," Nat. Methods **8**, 1044–1046 (2011).
58. M. Friedrich, Q. Gan, V. Ermolayev, and G. S. Harms, "STED–SPIM: stimulated emission depletion improves sheet illumination microscopy resolution," Biophys. J. **100**, L43–L45 (2011).
59. S. T. Hess, T. P. K. Girirajan, and M. D. Mason, "Ultra-high resolution imaging by fluorescence photoactivation localization microscopy," Biophys. J. **91**, 4258–4272 (2006).
60. B. Huang, W. Wang, M. Bates, and X. Zhuang, "Three-dimensional super-resolution imaging by stochastic optical reconstruction microscopy," Science **319**, 810–813 (2008).
61. R. Galland, G. Grenci, A. Aravind, V. Viasnoff, V. Studer, and J.-B. Sibarita, "3D high- and super-resolution imaging using single-objective SPIM," Nat. Methods **12**, 641–644 (2015).
62. T. Bruns, S. Schickinger, R. Wittig, and H. Schneckenburger, "Preparation strategy and illumination of three-dimensional cell cultures in light sheet-based fluorescence microscopy," J. Biomed. Opt. **17**, 1015181 (2012).
63. R. Regmi, K. Mohan, and P. P. Mondal, "High resolution light-sheet based high-throughput imaging cytometry system enables visualization of intra-cellular organelles," AIP Adv. **4**, 097125 (2014).
64. H. Deschout, K. Raemdonck, S. Stremersch, P. Maoddi, G. Mernier, P. Renaud, S. Jiguet, A. Hendrix, M. Bracke, R. Van den Broecke, M. Roding, M. Rudemo, J. Demeester, S. C. De Smedt, F. Strubbe, K. Neyts, and K. Braeckmans, "On-chip light sheet illumination enables diagnostic size and concentration measurements of membrane vesicles in biofluids," Nanoscale **6**, 1741–1747 (2014).
65. P. Paiè, F. Bragheri, A. Bassi, and R. Osellame, "Selective plane illumination microscopy on a chip," Lab Chip **16**, 1556–1560 (2016).
66. P. Paiè, F. Bragheri, T. Claude, and R. Osellame, "Optofluidic light modulator integrated in lab-on-a-chip," Opt. Express **25**, 7313–7323 (2017).
67. E. Zagato, T. Brans, S. Verstuyft, D. van Thourhout, J. Missinne, G. van Steenberge, J. Demeester, S. De Smedt, K. Remaut, K. Neyts, and K. Braeckmans, "Microfabricated devices for single objective single plane illumination microscopy (SoSPIM)," Opt. Express **25**, 1732–1745 (2017).
68. M. B. M. Meddens, S. Liu, P. S. Finnegan, T. L. Edwards, C. D. James, and K. A. Lidke, "Single objective light-sheet microscopy for high-speed whole-cell 3D super-resolution," Biomed. Opt. Express **7**, 2219–2236 (2016).
69. V. Bianco, B. Mandracchia, V. Marchesano, V. Pagliarulo, F. Olivieri, S. Coppola, M. Paturzo, and P. Ferraro, "Endowing a plain fluidic chip with micro-optics: a holographic microscope slide," Light Sci. Appl. **6**, e17055 (2017).
70. D. Psaltis, S. R. Quake, and C. Yang, "Developing optofluidic technology through the fusion of microfluidics and optics," Nature **442**, 381–386 (2006).
71. S. A. Lee, R. Leitao, G. Zheng, S. Yang, A. Rodriguez, and C. Yang, "Color capable sub-pixel resolving optofluidic microscope and its application to blood cell imaging for malaria diagnosis," PLOS ONE **6**, e26127 (2011).
72. X. Shi and L. Hesselink, "Mechanisms for enhancing power throughput from planar nano-apertures for near-field optical data storage," Jpn. J. Appl. Phys. **41**, 1632–1635 (2002).
73. A. Greenbaum, W. Luo, B. Khademhosseinieh, T.-W. Su, A. F. Coskun, and A. Ozcan, "Increased space-bandwidth product in pixel super-resolved lensfree on-chip microscopy," Sci. Rep. **3**, 1717 (2013).
74. L. M. Lee, X. Cui, and C. Yang, "The application of on-chip optofluidic microscopy for imaging *Giardia lamblia* trophozoites and cysts," Biomed. Microdevices **11**, 951–958 (2009).
75. G. Zheng, S. A. Lee, S. Yang, and C. Yang, "Sub-pixel resolving optofluidic microscope for on-chip cell imaging," Lab Chip **10**, 3125–3129 (2010).
76. S. Pang, C. Han, L. M. Lee, and C. Yang, "Fluorescence microscopy imaging with a Fresnel zone plate array based optofluidic microscope," Lab Chip **11**, 3698–3702 (2011).
77. M. Sanz, J. Á. Picazo-Bueno, L. Granero, J. García, and V. Micó, "Compact, cost-effective and field-portable microscope prototype based on MISHELF microscopy," Sci. Rep. **7**, 43291 (2017).
78. W. Bishara, T. W. Su, A. F. Coskun, and A. Ozcan, "Lensfree on-chip microscopy over a wide field-of-view using pixel super-resolution," Opt. Express **18**, 11181–11191 (2010).
79. W. Bishara, U. Sikora, O. Mudanyali, T. W. Su, O. Yaglidere, S. Luckhart, and A. Ozcan, "Holographic pixel super-resolution in portable lensless on-chip microscopy using a fiber-optic array," Lab Chip **11**, 1276–1279 (2011).
80. A. Greenbaum, Y. Zhang, A. Feizi, P.-L. Chung, W. Luo, S. R. Kandukuri, and A. Ozcan, "Wide-field computational imaging of pathology slides using lens-free on-chip microscopy," Sci. Transl. Med. **6**, 267ra175 (2014).
81. W. Luo, A. Greenbaum, Y. Zhang, and A. Ozcan, "Synthetic aperture-based on-chip microscopy," Light Sci. Appl. **4**, e261 (2015).
82. A. Greenbaum, A. Feizi, N. Akbari, and A. Ozcan, "Wide-field computational color imaging using pixel super-resolved on-chip microscopy," Opt. Express **21**, 12469–12483 (2013).
83. Y. Zhang, Y. Wu, Y. Zhang, and A. Ozcan, "Color calibration and fusion of lens-free and mobile-phone microscopy images for high-resolution and accurate color reproduction," Sci. Rep. **6**, 27811 (2016).
84. M. M. Villone, G. D'Avino, M. A. Hulsen, and P. L. Maffettone, "Dynamics of prolate spheroidal elastic particles in confined shear flow," Phys. Rev. E **92**, 062303 (2015).
85. F. Merola, P. Memmolo, L. Miccio, R. Savoia, M. Mugnano, A. Fontana, G. D'Ippolito, A. Sardo, A. Iolascon, A. Gambale, and P. Ferraro, "Tomographic flow cytometry by digital holography," Light Sci. Appl. **6**, e16241 (2017).
86. C. Faigle, F. Lautenschläger, G. Whyte, P. Homewood, E. Martín-Badosa, and J. Guck, "A monolithic glass chip for active single-cell sorting based on mechanical phenotyping," Lab Chip **15**, 1267–1275 (2015).
87. C. Liberale, G. Cojoc, F. Bragheri, P. Minzioni, G. Perozziello, R. La Rocca, L. Ferrara, V. Rajamanickam, E. Di Fabrizio, and I. Cristiani, "Integrated microfluidic device for single-cell trapping and spectroscopy," Sci. Rep. **3**, 1258 (2013).
88. Y. Z. Shi, S. Xiong, L. K. Chin, Y. Yang, J. B. Zhang, W. Ser, J. H. Wu, T. N. Chen, Z. C. Yang, Y. L. Hao, B. Liedberg, P. H. Yap, Y. Zhang, and A. Q. Liu, "High-resolution and multi-range particle separation by microscopic vibration in an optofluidic chip," Lab Chip **17**, 2443–2450 (2017).
89. B. H. Wunsch, J. T. Smith, S. M. Gifford, C. Wang, M. Brink, R. L. Bruce, R. H. Austin, G. Stolovitzky, and Y. Astier, "Nanoscale lateral displacement arrays for the separation of exosomes and colloids down to 20 nm," Nat. Nanotechnol. **11**, 936–940 (2016).
90. S. H. Ko, D. Chandra, W. Ouyang, T. Kwon, P. Karande, and J. Han, "Nanofluidic device for continuous multiparameter quality assurance of biologics," Nat. Nanotechnol. **12**, 804–812 (2017).
91. A. K. Lau, H. C. Shum, K. K. Wong, and K. K. Tsia, "Optofluidic time-stretch imaging—an emerging tool for high-throughput imaging flow cytometry," Lab Chip **16**, 1743–1756 (2016).
92. K. Goda, K. K. Tsia, and B. Jalali, "Serial time-encoded amplified imaging for real-time observation of fast dynamic phenomena," Nature **458**, 1145–1149 (2009).
93. F. Xing, H. Chen, C. Lei, Z. Weng, M. Chen, S. Yang, and S. Xie, "Serial wavelength division 1 GHz line-scan microscopic imaging," Photon. Res. **2**, B31–B34 (2014).
94. A. M. Fard, A. Mahjoubfar, K. Goda, D. R. Gossett, D. Di Carlo, and B. Jalali, "Nomarski serial time-encoded amplified microscopy for high-speed contrast-enhanced imaging of transparent media," Biomed. Opt. Express **2**, 3387–3392 (2011).
95. K. Goda, A. Ayazi, D. R. Gossett, J. Sadasivam, C. K. Lonappan, E. Sollier, A. M. Fard, S. C. Hur, J. Adam, C. Murray, C. Wang, N. Brackbill, D. Di Carlo, and B. Jalali, "High-throughput single-microparticle imaging flow analyzer," Proc. Natl. Acad. Sci. USA **109**, 11630–11635 (2012).
96. T. T. W. Wong, A. K. S. Lau, K. K. Y. Ho, M. Y. H. Tang, J. D. F. Robles, X. Wei, A. C. S. Chan, A. H. L. Tang, E. Y. Lam, K. K. Y. Wong, G. C. F. Chan, H. C. Shum, and K. K. Tsia, "Asymmetric-detection time-stretch optical microscopy (ATOM) for ultrafast high-contrast cellular imaging in flow," Sci. Rep. **4**, 3656 (2014).
97. M. Ugawa, C. Lei, T. Nozawa, T. Ideguchi, D. Di Carlo, S. Ota, Y. Ozeki, and K. Goda, "High-throughput optofluidic particle profiling with morphological and chemical specificity," Opt. Lett. **40**, 4803–4806 (2015).